

---

**Technical Report No: ND08-04**

**Selected Pesticide Remediation with Iron Nanoparticles:  
Modeling and Barrier Applications**

by

**Jay M. Thompson  
Achintya N. Bezbaruah**

**Dept. of Civil Engineering, North Dakota State University  
Fargo, North Dakota  
September, 2008**

**North Dakota Water Resources Research Institute  
North Dakota State University, Fargo, North Dakota**

## **Technical Report No: ND08-04**

# **Selected Pesticide Remediation with Iron Nanoparticles: Modeling and Barrier Applications**

by

Jay M. Thompson<sup>1</sup>

Achintya N. Bezbaruah<sup>2</sup>

<sup>1</sup>  
WRI Graduate Research Fellow and Assistant Professor<sup>2</sup>  
Department of Civil Engineering  
North Dakota State University  
Fargo, ND 58105  
September, 2008

*The work upon which this report is based was supported in part by federal funds provided by the United States of Department of Interior in the form of ND WRI Graduate Research Fellowship for the graduate student through the North Dakota Water Resources Research Institute.*

*Contents of this report do not necessarily reflect the views and policies of the US Department of Interior, nor does mention of trade names or commercial products constitute their endorsement or recommendation for use by the US government.*

**Project Period: March 1, 2007 – August 31, 2008**  
**Project Numbers: 2007ND149B and 2008ND165B**

**North Dakota Water Resources Research Institute**  
**Director, G. Padmanabhan**  
**North Dakota State University**

## TABLE OF CONTENTS

LIST OF TABLES .....	v
LIST OF FIGURES .....	v
ABSTRACT.....	1
ACKNOWLEDGEMENTS.....	2
BACKGROUND .....	3
Remediation with Zero-valent Iron.....	3
Nanoscale Zero-valent Iron.....	3
Alachlor, Atrazine, Dicamba and Picloram.....	4
DESCRIPTION OF THE STATE OR REGIONAL WATER PROBLEM INVESTIGATED .....	4
SCOPE AND OBJECTIVES.....	4
MATERIALS AND METHODS.....	7
Chemicals.....	7
Iron Nanoparticle Synthesis.....	7
Iron Nanoparticle Characterization.....	7
nZVI-alginate Synthesis.....	8
Batch Study 1: Alachlor and Atrazine Degradation by nZVI.....	8
Batch Study 2: Alachlor Degradation by mZVI .....	9
Batch Study 3: Alachlor Degradation Under Different Ionic Strengths .....	9
Batch Study 4: Mixed Pesticide Degradation in Alginate-nZVI System .....	9
Analytical Methods.....	10

RESULTS AND DISCUSSION .....	10
Iron Nanoparticle Characterization.....	10
Reaction Kinetics .....	10
Batch Study 1: Alachlor and Atrazine Degradation by nZVI .....	13
Batch Study 2: Alachlor Degradation by mZVI.....	14
Batch Study 3: Alachlor Degradation Under Different Ionic Strengths .....	16
Batch Study 4: Mixed Pesticide Degradation in Alginate-nZVI System .....	17
Reaction By-product(s) .....	17
CONCLUSIONS.....	17
REFERENCES .....	19

## LIST OF TABLES

Table 1. Properties of alachlor, atrazine, dicamba and picloram (USDA, 2007) .....	5
Table 2. Summary of alachlor degradation kinetics .....	16

## LIST OF FIGURES

Figure 1. TEM image of iron nanoparticle cluster.....	11
Figure 2. Magnified view of TEM image .....	12
Figure 3. Size distribution of synthesized iron nanoparticles .....	12
Figure 4. XRD spectrum of synthesized iron nanoparticles .....	13
Figure 5. Data from alachlor degradation study (Batch Study 1).....	15
Figure 6. Chloride mass balance for alachlor degradation by nZVI.....	15
Figure 7. Comparison of observed alachlor degradation reaction rate constant under different ionic strength conditions .....	16
Figure 8. Reduction of alachlor in alginate-nZVI system.....	18

## ABSTRACT

Pesticide contamination of groundwater is a major concern in agricultural areas. Of the many remediation technologies developed in the last decade, zero-valent iron is among the most studied. Nanoscale zero-valent iron (nZVI), with its unique properties and high surface area, enhances many of the advantages of traditional iron remediation. Unfortunately, studies comprehensively examining the utility of iron nanoparticles for pesticide remediation are lacking. The intent of this work is to survey the effectiveness of iron nanoparticles for several common chlorinated pesticides and to comprehensively study the reaction kinetics. Specifically, this study examined the effectiveness of iron nanoparticles for the treatment of the herbicides alachlor, atrazine, dicamba and picloram.

Iron nanoparticles were synthesized by the borohydride reduction method and characterized using transmission electron microscopy, X-ray diffraction and Brunauer-Emmett-Teller (BET) specific surface area analysis. The resulting particles had an average diameter of 35 nm and a N<sub>2</sub>-BET specific surface area of 25 m<sup>2</sup> g<sup>-1</sup>. Of the compounds studied, only alachlor degraded in the presence of nZVI.

The surface area normalized pseudo first-order rate constant ( $k_{SA}$ ) for alachlor dechlorination by nZVI was found to be  $38.5 \times 10^{-5} \text{ L h}^{-1} \text{ m}^{-2}$  ( $R^2 = 0.999$ ). The primary reaction by-product was identified as dechlorinated alachlor. The effect of ionic strength was also examined. The results suggested that nZVI might be a viable option for both site remediation and low volume, high concentration pesticide waste treatment.

## **ACKNOWLEDGEMENTS**

Stipend support and supplemental funding from the North Dakota Water Resources Institute are thankfully acknowledged. The authors also wish to recognize the North Dakota State University Development Foundation for funding portions of this work. The authors are grateful to Dr. Scott Korom and Hanying Xu (University of North Dakota) and Anuradee Witthayapanyanon (University of Oklahoma) for their assistance in ion chromatography and BET analysis, respectively.

## BACKGROUND

### *Remediation with Zero-valent Iron*

The zero-valent iron remediation process is generally a two-electron redox reaction. The standard electrode potential of the zero-valent iron/ferrous iron system is -0.44 V (Milazzo et al., 1978). A number of environmentally relevant compounds, most notably chlorinated aliphatic compounds, are sufficiently oxidized to yield a thermodynamically favorable oxidation-reduction reaction with zero-valent iron (Johnson et al., 1996). Matheson and Tratnyek (1994) have identified the following reaction:



The advantages of iron metal for remediation include its non-toxicity, and economy. Lab-scale studies on iron (in the form of filings or microscale powder) have been successful in treating chlorinated ethanes (Orth and Gillham, 1996; Hara et al., 2005), chlorinated methanes (Matheson and Tratnyek, 1994), arsenic (Luepin et al., 2005). Traditional zero-valent iron (non-nano) has been employed in hundreds of sites, usually in the form of permeable barriers (Rock et al., 1998). Numerous detailed performance evaluations of permeable barriers have proven the technology effective (Phillips et al., 2000; Morrison, et al., 2001; Wilkin et al., 2005).

### *Nanoscale Zero-valent Iron*

Weber (1996) showed that zero-valent iron redox reactions are surface mediated. Thus, reaction rates can be improved by increasing the available iron surface area. Nanoscale zero-valent iron (nZVI) can drastically improve reaction rates, compared to microscale zero-valent iron, due to its high specific surface area (Zhang, 2003). Most iron nanoparticles used for environmental remediation have diameters in the range of 20-800 nm (Li et al., 2006). Iron nanoparticles have specific surface areas on the order of 20-30  $\text{m}^2\text{g}^{-1}$  (Zhang, 2003) compared to about  $< 2 \text{ m}^2\text{g}^{-1}$  for traditional iron (Sigma-Aldrich, 2007). There is still significant debate as to whether the enhanced reaction rates are mainly due only to surface area (Nurmi et al., 2005) or if there are some other properties intrinsic only to iron nanoparticles. Liu et al. (2005b) posit that borohydride synthesized (a wet chemistry method that is very well-researched) iron nanoparticles have the unique property to activate  $\text{H}_2$ , promoting hydrodehalogenation and hydrogenation. While a wide variety of nZVI synthesis techniques (Li et al., 2006 list four physical methods and seven chemical methods all producing, sometimes wide, differences in physical properties), this work will focus exclusively on borohydride synthesized particles.

Perhaps more important than nZVI enhanced reactivity is its potential to be directly injected into the subsurface. This potential has not yet been fully realized for nZVI (Quinn et al., 2005; Saleh et al., 2008) due to its limited mobility in the subsurface. Nanoscale iron subsurface mobility is limited by particle-soil grain attachment and particle-particle agglomeration (Saleh et al., 2007). To increase subsurface mobility

nZVI is mixed with surfactants (Saleh et al., 2008) or, more frequently, coated with polymers (Saleh et al., 2005; Hydutsky et al., 2007; Krajangpan et al., 2008).

While there has been very limited study on pesticide degradation by bimetallic (Pd-Fe) iron nanoparticles (Joo and Zhao, 2007), no work has yet been reported on pesticide degradation in anoxic condition in the presence of only nZVI.

### ***Alachlor, Atrazine, Dicamba and Picloram***

The pesticide compounds tested in this study were selected on the basis of an extensive review of the Fe<sup>0</sup> reductive dechlorination literature. The four compounds selected (Table 1), alachlor, atrazine, dicamba and picloram, have been shown by previous researchers to be susceptible to Fe<sup>0</sup> reductive dechlorination (Eykholt and Davenport, 1998; Ghauch and Suptil, 2000; Dombeck et al., 2001; Ghauch, 2001; Gibb et al., 2004). No comprehensive kinetic studies have been conducted on the above compounds with iron nanoparticles.

## **DESCRIPTION OF THE STATE OR REGIONAL WATER PROBLEM INVESTIGATED**

Sixty percent of North Dakota's population uses groundwater as their drinking water source (Radig, 1997). In rural areas, 97% of the population depends on groundwater (Radig, 2006). Protection of this resource is of vital interest to the people of North Dakota.

Modern agricultural practice has prevented high-level non-point source contamination of ground water (Koplin 1998). While vigilance must be maintained on non-point source contamination, a more immediate problem is the point source contamination of groundwater at agricultural chemical retail outlets and pesticide storage, mixing, and loading facilities on farms. North Dakota water quality officials cite the release of the herbicides used to control leafy spurge, such as dicamba, at these retail outlets (Bartelson, 2006). In Minnesota, the most common pesticide contamination scenario is the accidental release of corn herbicides at agricultural chemical retail outlets (Villas-Horn, 2006). The development of new pesticide spill remediation technologies can potentially abate these issues.

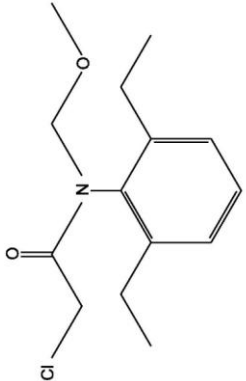
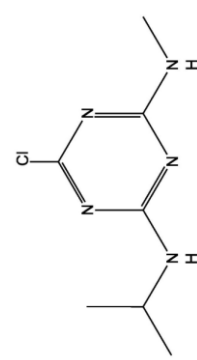
## **SCOPE AND OBJECTIVES**

The broad objective of this research is to determine the efficacy of zero-valent iron (Fe<sup>0</sup>) nanoparticles (nZVI) for remediation of a spectrum of widely used pesticides. Further, the reaction kinetics will be quantified and modeled.

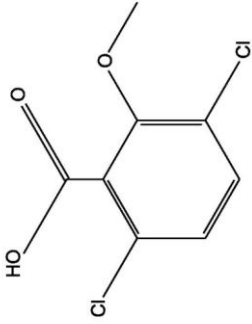
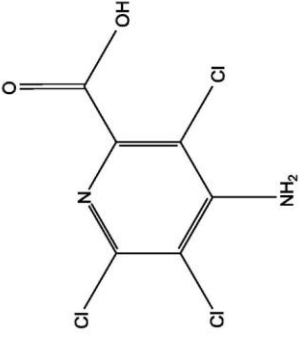
The specific objectives of this research are as follows:

- (a) Determine if nZVI is effective in treating atrazine, alachlor, dicamba and picloram.

**Table 1.** Properties of alachlor, atrazine, dicamba and picloram (USDA, 2007).

	<b>Structure</b>	<b>Chemical Formula</b>	<b>Molecular Weight</b>	<b>H<sub>2</sub>O Solubility<sup>(a)</sup></b>	<b>K<sub>ow</sub></b>	<b>K<sub>oc</sub></b>	<b>Soil T<sub>1/2</sub><sup>(b)</sup></b>
<b>Alachlor</b>		$C_{14}H_{20}ClNO_2$	269.8	240 mg L <sup>-1</sup>	794	124	21 d
<b>Atrazine</b>		$C_8H_{14}ClN_5$	215.7	33 mg L <sup>-1</sup>	479	147	77-146 d

**Table 1.** (continued)

	Structure	Chemical Formula	Molecular Weight	H <sub>2</sub> O Solubility <sup>(a)</sup>	K <sub>OW</sub>	K <sub>OC</sub>	Soil T <sub>1/2</sub> <sup>(b)</sup>
<b>Dicamba</b>		C <sub>8</sub> H <sub>6</sub> Cl <sub>2</sub> O <sub>3</sub>	215.7	8310 mg L <sup>-1</sup>	3.6	13	18 d
<b>Picloram</b>		C <sub>6</sub> H <sub>3</sub> Cl <sub>3</sub> N <sub>2</sub> O <sub>2</sub>	241.5	430 mg L <sup>-1</sup>	1.1	29	18-300 d <sup>(c)</sup>

<sup>(a)</sup> At 25° C. <sup>(b)</sup> Half-life in soil is highly dependent on microbial/soil conditions; a typical value is presented. <sup>(c)</sup> Half-life is highly dependent on picloram concentration.

- (b) If applicable, quantify the reaction kinetics of pesticide degradation by nZVI.
- (c) Determine the effect, if any, of ionic strength on reaction kinetics of pesticide degradation by nZVI.
- (d) Develop a simple, biocompatible subsurface delivery vehicle for the nZVI.

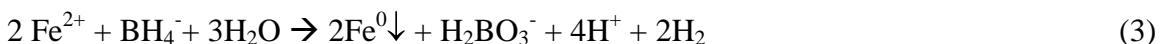
## MATERIALS AND METHODS

### *Chemicals*

All materials were used as received. Chemicals were stored at room temperature (22±2°C) except pesticide standards (stored at -18°C) and pesticide stock solutions (stored at 4°C). Pesticide stock solutions were replaced every month

### *Iron Nanoparticle Synthesis*

Nanoscale zero-valent iron particles were synthesized by borohydride reduction of ferrous iron, which was modified slightly from a method by Liu et al. (2005a). The reaction scheme for the synthesis is as follows:



An aqueous solution of NaBH<sub>4</sub> (98%, Aldrich) was added drop-wise to a Fe(SO<sub>4</sub>)•7H<sub>2</sub>O (99%, Alfa Aesar) methanol/water solution resulting in a suspension of iron particles that was subsequently vacuum filtered and washed with copious amounts of ethanol to remove any excess borohydride. The iron was then dried using alternating exposures to nitrogen gas and vacuum at 120°C using standard Schlenk procedures. After thoroughly drying the iron, air was allowed to slowly bleed into the Schlenk flask over a period of approximately 12 h to passivate the iron. The resulting black clusters of iron were ground, yielding fine nZVI powder. The nZVI was stored in a nitrogen environment in a glovebox (Innovation Technology Inc.) for later use.

### *Iron Nanoparticle Characterization*

#### TEM Analysis

Particle morphology was characterized by transmission electron microscopy (TEM, JEOL JEM-100CX II). A concentrated nZVI sample was prepared in ethanol, sonicated, and placed on a Formvar<sup>®</sup> coated 300 mesh copper grid for analysis at an accelerating voltage of 80 kV. Some sample oxidation during preparation was unavoidable.

## XRD Analysis

X-ray diffraction (XRD) analysis of nZVI was performed on a Philips X'Pert MPD with Cu K $\alpha$  X-ray source. Sample was ground, dispersed in hexane set on a glass slide and analyzed upon evaporation of the hexane. Some sample oxidation during preparation was unavoidable. Analysis was carried out at 40 kV and 30 mA with a scan range from 20° to 80°.

## BET Specific Surface Area Analysis

Brunauer-Emmett-Teller (BET) specific surface area of nZVI was determined by N<sub>2</sub> gas absorption (Micromeritics, ASAP 2000). BET analysis was conducted at the University of Oklahoma (Norman, OK) following standard procedures (ASTM, 2004). Particles were analyzed with no further preparation. The surface area of microscale ZVI (mZVI) used in this study was supplied by the manufacturer.

## *nZVI-alginate Synthesis*

The intent of this experiment was to determine if entrapping nZVI in an alginate matrix will significantly reduce the alachlor reaction rate. The primary objective of this entrapment was a simple and inexpensive permeable reactive barrier technology. A method for entrapping cells (Asku et al., 1998) in alginate was modified for nZVI entrapment. One gram of sodium alginate was dissolved in 50 mL of deionized, deoxygenated (N<sub>2</sub> sparged) water. Great care was taken to minimize the introduction of oxygen into the solution while being stirred. The resulting viscous gel was then set aside for 30 minutes to allow any air bubbles to escape. A measured amount (1.0 g) of nZVI was then gently added into the gel which was kept stirred. The nZVI-alginate mixture was then dropped into a 3.5% (w/v) deoxygenated CaCl<sub>2</sub> solution using a peristaltic pump. The alginate-nZVI immediately formed spherical beads upon contact with the CaCl<sub>2</sub> solution. Beads were immersed in the CaCl<sub>2</sub> solution for 9 hrs to facilitate hardening and ensure optimal diffusion characteristics (Garbayo et al., 2002).

## ***Batch Study 1: Alachlor and Atrazine Degradation by nZVI***

Batch studies examining the reaction kinetics of alachlor and atrazine with nZVI were conducted. Trials were conducted in 500 mL polyethylene terephthalate bottles with fluoropolymer resin-coated silicone septum screw caps.

Vials were covered with aluminum foil to prevent possible photodegradation (Bahena and Martínez, 2006). Deionized (Barnstead, 18 M $\Omega$ ) water (400 mL) was pipetted into the bottles and spiked with an alachlor (99.2%, Chem Service) stock solution (1.0 mg mL<sup>-1</sup> in methanol) at varying levels to yield 10-40 mg L<sup>-1</sup> pesticide solutions. The pesticide solution was then sparged with nitrogen gas (ultra high purity grade, ChemGas) to deoxygenate the solution. Samples were not withdrawn prior to sparging, thus the effects of volatilization were not considered in analysis. Initial pH (pH<sub>0</sub>)

≈ 6.0-8.0) was not adjusted and trials were not buffered. A measured amount (1.60 g) of nZVI was placed in each vial and the headspace was purged with nitrogen gas. After brief sonication to break any iron aggregates, trial, blank and control vials were placed on a custom built rotary shaker (28 rpm). Aliquots (2 mL) were periodically (0, 3, 6, 12, 24, 48 and 72 h) withdrawn by syringe and passed through a 0.02 μm pore size syringe filter (Whatman, Anatotop 10). Samples were stored at 4°C and analyzed within 48 h of collection. All trials in this batch study were conducted at room temperature (22±2°C) and run in triplicate unless otherwise specified. Control for this batch study was provided by a trial with identical conditions, excepting the addition of iron.

### ***Batch Study 2: Alachlor Degradation by mZVI***

Parallel comparison trials were conducted under identical conditions to Batch Study 1, replacing nZVI with 200 g of microscale zero-valent powder (99.9%, Aldrich). This mass was selected on the basis of non-rigorous trials to determine an appropriate mZVI mass that yielded kinetics similar to that observed in the nZVI trials. All trials in this batch study were conducted at room temperature (22±2°C) and run in triplicate unless otherwise specified.

### ***Batch Study 3: Alachlor Degradation Under Different Ionic Strengths***

A set of four trials was conducted to evaluate the effect of solution ionic strength on alachlor degradation kinetics. An alachlor solution (20 mg L<sup>-1</sup>) was prepared as previously described for Batch Study 1. The ionic strength of the solutions was adjusted to 10 mM (trials 1 and 2) and 100 mM (trials 3 and 4) with the addition of calcium chloride (CaCl<sub>2</sub> in trials 1 and 3) and sodium chloride (NaCl in trials 2 and 4). Experiments were carried out sacrificially in 20 mL borosilicate glass vials with fluoropolymer resin/silicone lined septum screw caps (EP Scientific Products). Vials were agitated in a custom built rotary shaker (28 rpm) at room temperature and samples were withdrawn, stored and analyzed as described earlier. All trials in this batch study were conducted at room temperature (22±2°C) and run in triplicate unless otherwise specified.

### ***Batch Study 4: Mixed Pesticide Degradation in Alginate-nZVI System***

A batch test examining the performance of nZVI entrapped in alginate beads was performed on a pesticide mixture solution containing alachlor, dicamba and picloram. Batch studies were carried out in a similar manner as in Batch Study 1. Each 500 mL polyethylene terephthalate bottle contained 400 mL of deoxygenated, deionized water spiked with alachlor, dicamba (99%, Chem Service), and picloram (99%, Chem Service) methanol solutions (all 2.5 g L<sup>-1</sup>) resulting in final concentrations of 10-20 mg L<sup>-1</sup> for each pesticide. The alginate-nZVI beads (1.0 g, by Fe weight) were then placed in the bottles. Control and alginate-blank (no Fe) trials were also performed. Samples were withdrawn at 0, 3, 6, 12, 24, 48, 72, 120 hrs. All trials in this batch study were conducted at room temperature (22±2°C) and run in triplicate unless otherwise specified. Controls and blanks for this batch study were provided by trials with identical conditions,

excepting the inclusion of alginate-nZVI and excepting the inclusion of nZVI into the alginate matrix, respectively.

## ***Analytical Methods***

### **HPLC Method**

Aqueous alachlor concentration was analyzed by reverse phase HPLC (1100 Series, Agilent Technologies) using a C-18 column (ZORBAX RX-C18, 5  $\mu\text{m}$ , 4.6 x 250 mm, Agilent Technologies) and diode array detector. The mobile phase consisted of 40:60 water to acetonitrile at a flow rate of 1.0 mL  $\text{min}^{-1}$ . Detection was achieved at 222 nm with a retention time of 8.10 min.

The HPLC method was modified as follows for dicamba and picloram analysis. The mobile phase consisted of 60:40 0.4% triethanolamine (TEA) in water (pH = 7.5) to ACN. Picloram and dicamba peaks eluted at 2.36 and 3.33 minutes, respectively. The mobile phase for atrazine analysis was modified to 60:40 water:ACN. Atrazine was detected at 8.76 minutes.

### **GC-MS Method**

By-products of pesticide degradation by nZVI were identified using GC-MS (6890 Plus, HP; 5973 MSD, HP) equipped with a fused silica capillary column (ZB-35, 30.0 m x 250  $\mu\text{m}$  x 0.25  $\mu\text{m}$ , Phenomenex). Aqueous samples (10 mL) were extracted with 1 mL dichloromethane. Extracts were injected in the splitless mode with the inlet maintained at 250°C. Oven conditions were as follows: 50°C (hold 1 min) and increase 20°C  $\text{min}^{-1}$  to 280°C (hold 10.5 min). The carrier gas (He) flow rate was maintained at 1.0 mL  $\text{min}^{-1}$ .

### **Ion Chromatography Method**

Chloride ion concentration was determined by ion chromatography (IC) analysis (DX-120, Dionex) with an IonPac AS14 anion exchange column (4 x 250 mm, Dionex) and a conductivity detector. The eluent consisted of 3.5 mM  $\text{Na}_2\text{CO}_3$  and 1.0 mM  $\text{NaHCO}_3$  at a flow rate of 1.16 mL  $\text{min}^{-1}$ .

## **RESULTS AND DISCUSSION**

### ***Iron Nanoparticle Characterization***

Particle morphology and size were determined by TEM (Figures 1 and 2). Average particle diameter was determined to be approximately 35 nm (Figure 3). Past studies have reported similar average particle diameters (30-50 nm Li et al., 2006). A

thin (2-5 nm) oxide shell (Figure 2) was formed during particle passivation. This core/shell geometry has been reported earlier (Nurmi et al., 2005; Li et al., 2006). Again, this is in agreement with earlier shell thickness reports of 2.3-3.4 nm (Nurmi et al., 2005),

BET surface area was found to be  $25 \text{ m}^2 \text{ g}^{-1}$ . This value is in agreement with others who used similar nZVI synthesis techniques ( $22 \text{ m}^2 \text{ g}^{-1}$ , Ponder et al., 2000 and  $36 \text{ m}^2 \text{ g}^{-1}$ , Liu et al., 2005a). The observed BET specific surface area is also quite close to the theoretical specific surface area of  $22 \text{ m}^2 \text{ g}^{-1}$ , assuming spherical nZVI particle geometry:

$$SSA = \frac{6}{\rho d}, \quad (4)$$

where

SSA = specific surface area ( $\text{m}^2 \text{ g}^{-1}$ )

$\rho$  = bulk density of iron ( $7.87 \times 10^6 \text{ g m}^{-3}$ )

$d$  = average particle diameter ( $35 \times 10^{-9} \text{ m}$ )

The close agreement between the theoretical spherical SSA and BET determined SSA confirms the spherical particle geometry observed in TEM imaging and suggests a relatively smooth surface. XRD spectrum is presented in Figure 4. Only  $\text{Fe}^0$  was detected.

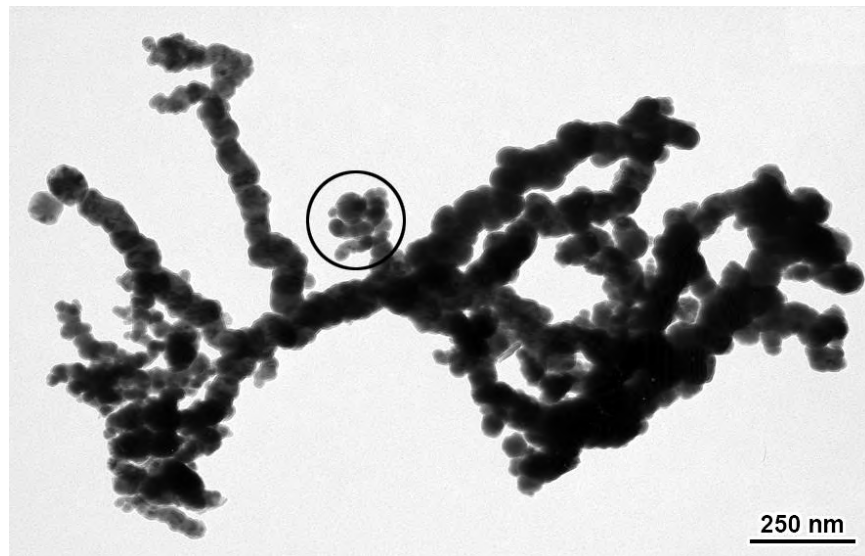


**Figure 1.** TEM image of iron nanoparticle cluster. The circled area is magnified in Figure 2.

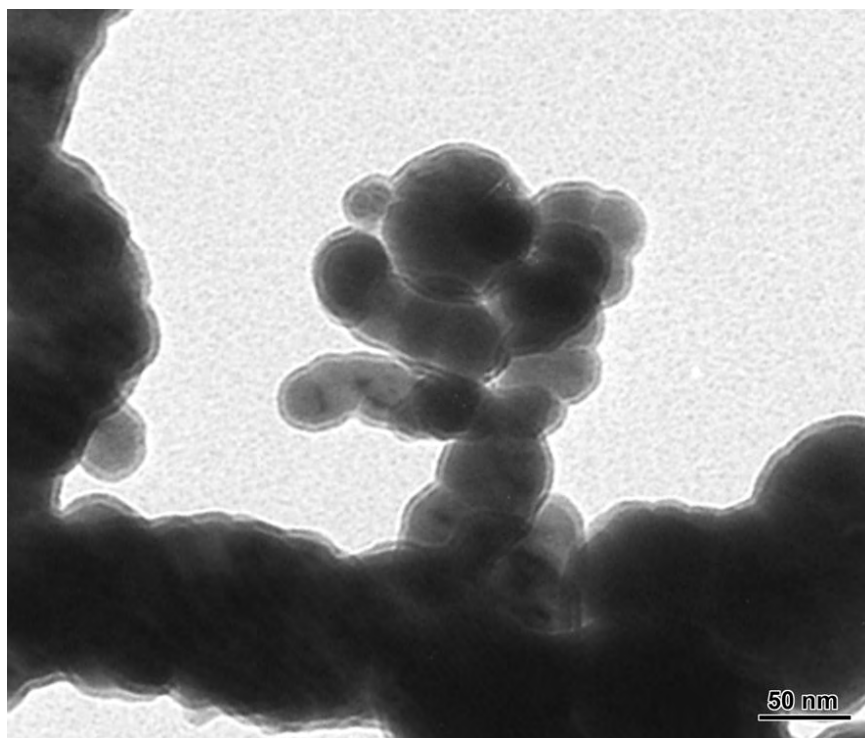


**Figure 2.** Magnified view of TEM image. Area is indicated in Figure 1. A thin layer (2-5 nm) of oxide was formed during particle passivation.

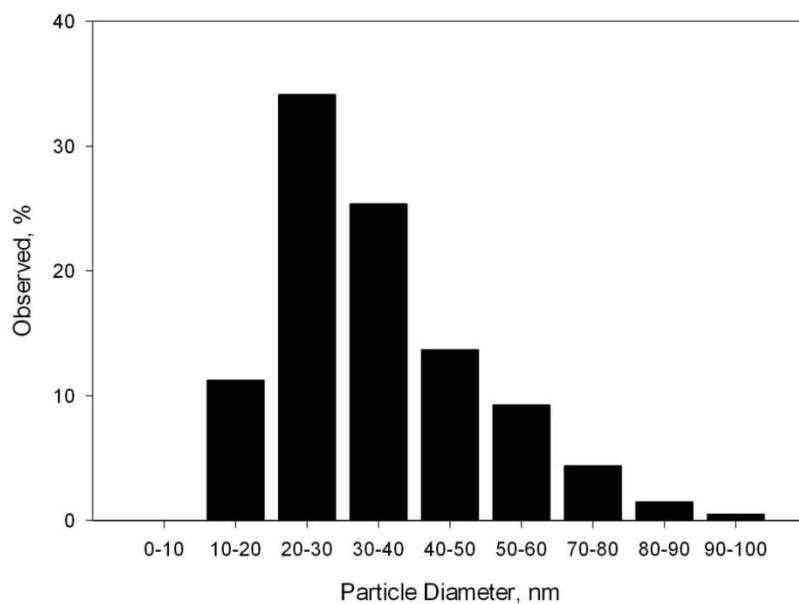


**Figure 3.** Size distribution of synthesized iron nanoparticles (sample size,  $n \approx 200$ ).

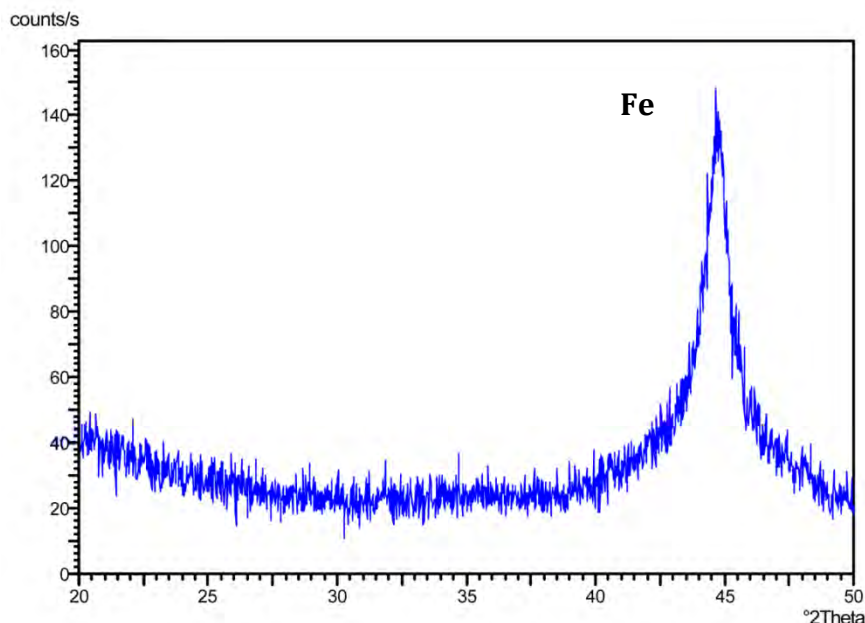


**Figure 4.** XRD spectrum of synthesized iron nanoparticles. Only Fe peak could be observed.

### ***Reaction Kinetics***

Degradation of the pesticides by nZVI was the primary interest of this study. No appreciable degradation of atrazine, dicamba or picloram was observed while rapid alachlor degradation was achieved.

#### **Batch Study 1: Alachlor and Atrazine Degradation by nZVI**

In Batch Study 1, atrazine did not degrade during the study period. Appreciable alachlor degradation was observed during the study period. The alachlor degradation reaction was found to obey first-order kinetics. This is common for the dehalogenation of organic compounds by both mZVI and nZVI (Johnson et al., 1996; Nurmi et al., 2005). The classical first-order rate reaction is

$$\frac{dC}{dt} = k_{obs} C, \quad (5)$$

where

$C$  = alachlor concentration ( $\text{mg L}^{-1}$ )  
 $k_{obs}$  = the observed rate constant ( $\text{h}^{-1}$ ).

In the case of heterogeneous reactions, such as ZVI-mediated dehalogenation, it is instructive to normalize  $k_{obs}$  with respect to (iron) surface area. It is believed that normalizing reaction rate with respect to surface area allows for more valid comparisons with different sized iron particles (Johnson et al., 1996; Nurmi et al., 2005).

While some do dissent from this view with respect to nanoparticles (Liu et al., 2005) due to observations that all (not only surface) of the nZVI particle iron is available for reaction, most researcher report nanoscale iron reaction rate constants on a surface area normalized basis. Johnson et al. (1996) have presented the following surface area normalized first-order rate equation:

$$\frac{dC}{dt} = k_{SA} \rho_A C, \quad (6)$$

where

$k_{SA}$  = surface area normalized rate constant ( $L m^{-2} h^{-1}$ )

$\rho_A$  = iron surface area per solution volume ( $m^2 L^{-1}$ ).

Also,

$$k_{OBS} = k_{SA} \rho_A \quad (7)$$

The proposed model was found to fit the collected data well ( $R^2 > 0.99$ ). The results from linear regression are summarized in Table 2. Modeling results are plotted in Figure 5.

An analysis of chloride ion ( $Cl^-$ ) concentration was conducted to both verify dechlorination and confirm chlorine mass balance. Chloride mass balance ranged from 94% to 98% (excluding the initial state, Figure 6). This small loss (2-6%) was considered acceptable and was attributed to instrumental and/or experimental error. The conversion of chlorine in alachlor to  $Cl^-$  strongly implies a reductive dechlorination degradation path.

### Batch Study 2: Alachlor Degradation by mZVI

Significant alachlor degradation was observed during the study period. The initial alachlor concentrations of  $20 mg L^{-1}$  (nominal), decreased to  $1.08 mg L^{-1}$  over the 72 h period indicating an average reaction efficiency of 95%.

Results of alachlor degradation by nZVI (Batch Study 1) were compared with results from this batch study (mZVI). The alachlor degradation results and nZVI and mZVI characteristics are summarized in Table 2. The surface area normalized rate constant,  $k_{SA}$ , was determined to be about 5-10 times greater for nZVI ( $k_{SA} = 38.5 \times 10^{-5} L m^{-2} h^{-1}$ ) than mZVI ( $k_{SA} = 3.85 - 7.7 \times 10^{-5} L m^{-2} h^{-1}$ ). While some degree of error in mZVI reaction rate determination is likely due to uncertainties in the manufacturer surface area estimate, this alone cannot account for the observed difference. Lien and Zhang (1999) observed an identical difference (~5 times) with respect to chlorinated methane degradation. This was attributed to the relative “freshness” of the synthesized nZVI compared with the commercial mZVI. Manufactured mZVI likely has significant crystalline oxide surface species, and, therefore, the available reactive surface area will be less than the BET surface area (Johnson et al., 1996). Given the similarities of the

present experimental setup and results with Lien and Zhang (1999), these inferences seem possible.

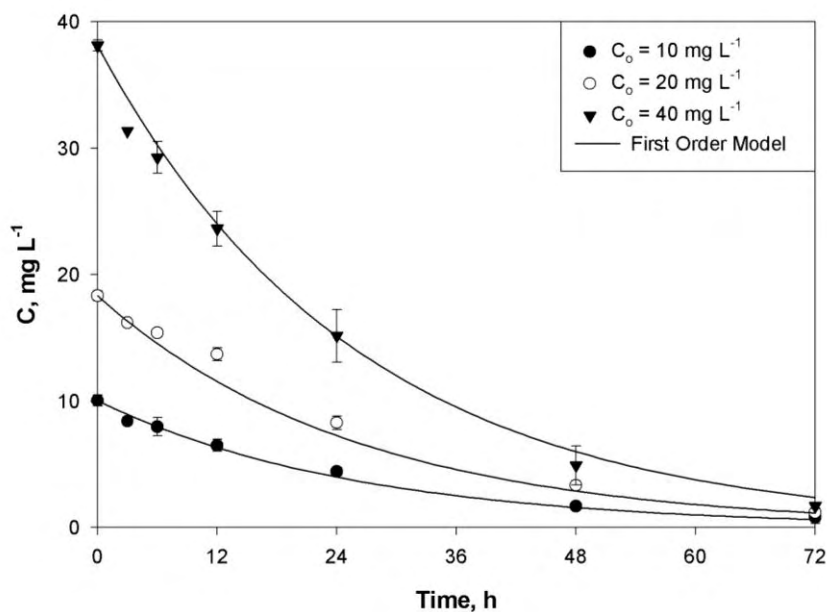


**Figure 5.** Data from alachlor degradation study (Batch Study 1). Degradation was modeled as a pseudo first-order reaction. The vertical error bars indicate  $\pm$  standard deviations.

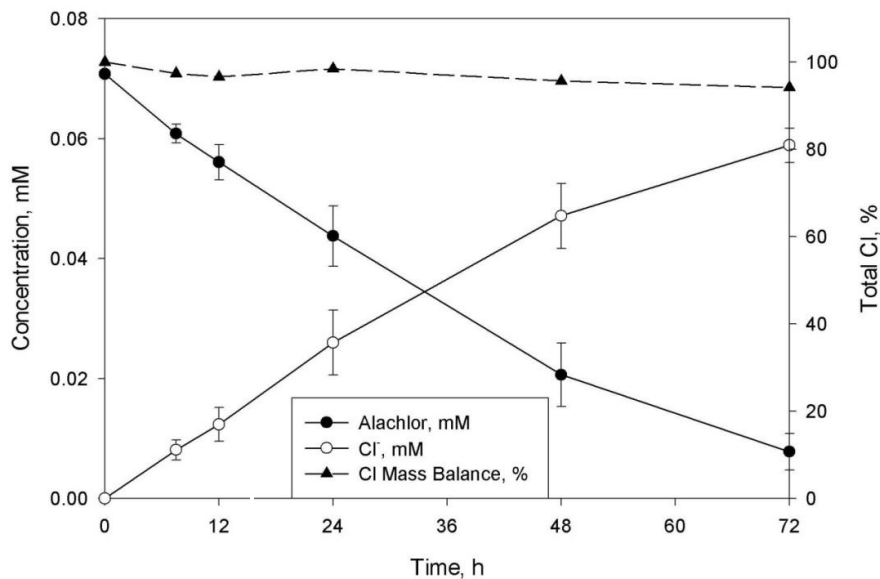


**Figure 6.** Chloride mass balance for alachlor degradation by nZVI. Chloride mass balance ranged from 94% to 98%. The vertical error bars indicate  $\pm$  standard deviations. Data points are joined by straight lines for ease of reading only and do not represent trends.

### Batch Study 3: Alachlor Degradation Under Different Ionic Strengths

Based on the results from Batch Studies 1, only alachlor was selected for degradation study under different ionic strength conditions. The degradation kinetics of alachlor by nZVI appears to be highly dependent on solution ionic strength. The surface area normalized rate constant ( $k_{SA}$ ) is reduced by roughly 90% upon the addition of either  $\text{CaCl}_2$  or  $\text{NaCl}$  equivalent to an ionic strength of 10 mM (Figure 7). There does not appear to be any significant difference in  $k_{SA}$  between  $\text{CaCl}_2$  and  $\text{NaCl}$ . Additions (100 mM) of the same salts do not affect  $k_{SA}$  beyond the values associated with 10 mM.

**Table 2.** Summary of alachlor degradation kinetics.  $\rho_A$  represents the iron surface area loading, i.e., iron surface area per solution volume.

Type of Iron	Average Diameter	Specific Surface Area ( $\text{m}^2 \text{g}^{-1}$ )	$\rho_A$ ( $\text{m}^2 \text{L}^{-1}$ )	$k_{\text{obs}}$ ( $\text{h}^{-1}$ )	$k_{SA}$ ( $\text{L m}^{-2} \text{h}^{-1}$ )	$R^2$
nZVI	35 nm	25	100	$38.5 \times 10^{-3}$	$38.5 \times 10^{-5}$	0.999
mZVI	3 $\mu\text{m}$	1-2 <sup>(a)</sup>	500-1000	$38.7 \times 10^{-3}$	$3.8 - 7.7 \times 10^{-5}$	0.987
Iron Filings <sup>(b)</sup>		1.4	496	$12.0 \times 10^{-2}$	$24.2 \times 10^{-5}$	

<sup>(a)</sup> Supplied by manufacturer (Sigma-Aldrich, 2007).

<sup>(b)</sup> Reported by Eykholt and Davenport (1998).

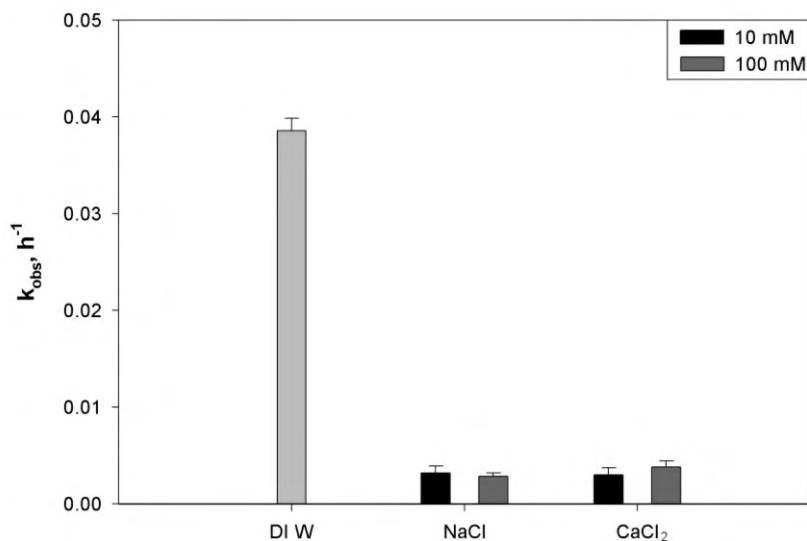


**Figure 7.** Comparison of observed alachlor degradation reaction rate constant under different ionic strength conditions. “DI W” stands for “deionized water”; trial has ionic strength of zero. Error bars represent 95% CI.

## Batch Study 4: Mixed Pesticide Degradation in Alginate-nZVI System

Alachlor was found to be reactive to nZVI-alginate. However, no transformation of dicamba or picloram was observed during the nZVI-alginate trial, although there was minimal diffusion into the alginate matrix. The reaction of nZVI-alginate with alachlor could be modeled as a pseudo first-order reaction with respect to iron surface (Figure 8). The effect of mass transfer resistance through alginate was neglected. The surface area normalized rate constant was found to be  $k_{SA} = 31.1 \times 10^{-5} \text{ L m}^{-2} \text{ h}^{-1}$  ( $R^2 = 0.984$ ). While the 95% confidence interval ( $\pm 5.0 \times 10^{-5}$ ) does not fall within the  $k_{SA}$  observed earlier for bare nZVI ( $38.5 \times 10^{-5} \text{ L m}^{-2} \text{ h}^{-1}$ ), the small discrepancy can probably be explained by the inherent variability between batches of synthesized nZVI and competition between alachlor and non-reactive pesticides for reactive sites on the iron surface.

It appears that alginate did not impede mass transfer to the iron in any meaningful manner. Pesticide losses due to alginate without iron were minimal. Thus, possible advantages of nZVI-alginate are feasible. Such secondary advantages may include use of alginate-entrapped nZVI in permeable reactive barriers and co-entrapment with pesticide degrading microorganisms.

### ***Reaction By-product(s)***

The GC-MS analysis was used for by-product identification. Only one by-product was detected and was identified by comparing its mass spectrum with that presented by Potter and Carpenter (1995). The by-product spectrum matched with that of dechlorinated alachlor (N-(2,6-Diethylphenyl)-N-(methoxymethyl)acetamide), providing further confirmation of reductive dechlorination. No other by-product was detected, and no attempt was made to quantify the identified by-product.

Comfort et al. (2001) working on the iron-mediated remediation of metolachlor (a structurally similar chloroacetanilide herbicide) found that dechlorinated metolachlor was five times more biodegradable than the parent compound. Thus, it seems likely that the dechlorination of alachlor results in some degree of improvement in biodegradability. Specific studies must be conducted before implementation to ensure the by-product is less toxic and/or persistent than the parent compound.

## **CONCLUSIONS**

Zero-valent iron nanoparticles were found to be effective in destroying alachlor and ineffective with respect to atrazine, dicamba and picloram. The authors contend nZVI can potentially be an effective remediation technique for select pesticides. However, successful use of nZVI for pesticide remediation will require an understanding of the properties, structure and reaction pathway for each pesticide, especially the position and bond strength of each halogen. Specific findings include:

- Alachlor degradation was found to be a pseudo first-order process. The surface area normalized rate constant was observed:  $k_{SA} = 38.5 \times 10^{-5} \text{ L m}^{-2} \text{ h}^{-1}$ . A comparison study with microscale iron particles found that nanoscale iron

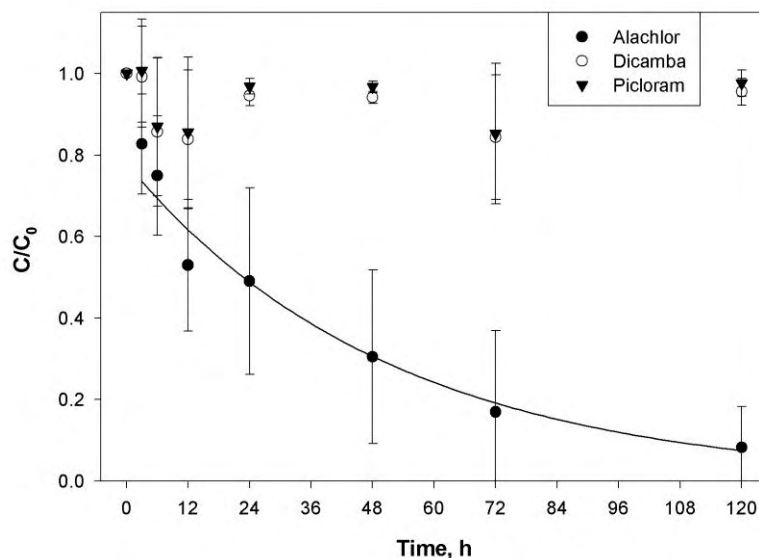


**Figure 8.** Reduction of alachlor in alginate-nZVI system. First data point is not considered in the model to account for initial diffusion into the alginate beads. The vertical error bars indicate  $\pm$  standard deviations.

- outperformed microscale iron by a factor of 5-10 in terms of surface area normalized reaction rate. This difference was attributed to oxide formation on the microscale iron.
- The reaction by-product of the alachlor-iron nanoparticle was found to be dechlorinated alachlor (N-(2,6-Diethylphenyl)-N-(methoxymethyl)acetamide). Although toxicity and persistence have not been characterized, a very similar compound was found to be more biodegradable than its parent compound. It is likely that dechlorinated alachlor will share this property.
- Ionic strength was found to have a large impact on alachlor-iron nanoparticles reaction kinetics. The surface area normalized rate constant,  $k_{SA}$ , was reduced by up to 90% at 10 mM ionic strength. Although no attempt was made to elucidate the cause of this  $k_{SA}$  reduction, previously published work suggests that the enhanced particle agglomeration associated with high ionic strength decrease the reaction rate.
- Iron nanoparticles entrapped in alginate were found to be equally effective in pesticide degradation as bare iron nanoparticles. Even though there was no enhancement in reaction rate in the alginate-nanoparticle system, the entrapment principle can possibly be used to retain the nanoparticles for a longer time in a treatment system (e.g., permeable reactive barrier).

## REFERENCES

- Aksu, Z., Egretli, G., Kutsal, T., 1998. A Comparative Study of Copper(II) Biosorption on Ca-Alginate, Agarose and Immobilized *C. Vulgaris* in a Packed Bed Column. *Process Biochem.* **33**, 393-400.
- ASTM, 2004. ASTM Standard C 33, Specification for Concrete Aggregates. ASTM International, West Conshohocken, PA.
- Bahena, C.L. and Martínez, S.S., 2006. Photodegradation of Chlorbromuron, Atrazine, and Alachlor in Aqueous Systems under Solar Irradiation. *Int. J. Photoenergy.* **Vol. 2006**, 1-6.
- Bartelson, N., North Dakota. Department of Health, Division of Water Quality, (Personal Communication). 2006.
- Comfort, S.D., Shea, P.J., Machacek, H.G., Oh, B.T., 2001. Field-Scale Remediation of a Metolachlor-Contaminated Spill Site Using Zerovalent Iron. *J. Environ. Qual.* **30**, 1636-1643.
- Dombeck, T, Dolan, E., Schultz, J., Klarup, D., 2001. Rapid Reductive Dechlorination of Atrazine by Zero-valent Iron Under Acidic Conditions. *Environ. Pollut.* **111**, 21-27.
- Eykholt, G.R., Davenport, D.T., 1998. Dechlorination of the Chloroacetanilide Pesticides Alachlor and Metolachlor by Iron Metal. *Environ. Sci. Technol.* **32**, 1482-1487.
- Garbayo, I., Leon, R., Vígara, J., Vylchez, C., 2002. Diffusion Characteristics of Nitrate and Glycerol in Alginate. *Colloid Surface* **B 25**, 1-9.
- Ghauch, A., Suptil, J., 2000. Remediation of S-Triazines Contaminated Water in a Laboratory Scale Apparatus using Zero-valent Iron Powder. *Chemosphere.* **41**, 1835-1843.
- Ghauch, A., 2001. Degradation of Benomyl, Picloram, and Dicamba in a Conical Apparatus by Zero-valent Iron Powder. *Chemosphere.* **43**, 1109-1117.
- Gibb, C., Satapanajaru, T., Comfort, S.D., Shea, P.J., 2004. Remediating Dicamba Contaminated-Water with Zerovalent Iron. *Chemosphere.* **54**, 841-848.
- Hara, J., Ito, H., Suto, K., Inoue, C., Chida, T., 2005. Kinetics of Trichloroethene Dechlorination with Iron Powder. *Wat. Res.* **39**, 1165-1173.
- Hydutsky, B.W., Mack, E.J., Beckerman, B.B., Skluzacek, J.M., Mallouk, T.E., 2007. Optimization of Nano- and Microiron Transport through Sand Columns Using Polyelectrolyte Mixtures. *Environ. Sci. Technol.* **41**, 6418-6424.
- Johnson, T.L., Scherer, M.M., Tratnyek, P.G., 1996. Kinetics of Halogenated Organic Compound Degradation by Iron Metal. *Environ. Sci. Technol.* **30**, 2634-2640.

- Joo, S.H., Zhao, D., 2007. Destruction of Lindane and Atrazine Using Stabilized Iron Nanoparticles Under Aerobic and Anaerobic Conditions: Effects of Catalyst and Stabilizer. *Chemosphere*. **70**, 418-425.
- Koplin, D.W., Barbash, J.E., Gilliom, R.J., 1998. Occurrence of Pesticides in Shallow Groundwater of the United States: Initial Results from the National Water-Quality Assessment Program. *Environ. Sci. Technol.* **32**, 558-566.
- Krajangpan, S., Jarabek, L., Jepperson, J., Chisholm, B., Bezbaruah, A., 2008. Polymer modified iron nanoparticles for environmental remediation. Proc. ACS Division of Polymeric Materials: Science & Engineering. New Orleans, LA. (pp. 22).
- Li, L., Fan, M., Brown, R.C., Van Leeuwen, J.H., Wang, J., Wang, W., Song, Y., Zhang, Z., 2006. Synthesis, Properties, and Environmental Applications of Nanoscale Iron-Based Materials: A Review. *Crit. Rev. Env. Sci. Tec.* **36**, 405-431.
- Lien, H.L., Zhang, W.X., 1999. Transformation of Chlorinated Methanes by Nanoscale Iron Particles. *J. Envir. Engrg.* **125**, 1042-1047.
- Liu, Y., Choi C., Dionysiou, D., Lowry, G. V., 2005a. TCE Hydrodechlorination by Amorphous Monometallic Nanoiron. *Chem. Mat.* **17**, 5315-5322
- Liu, Y., Majetich, S.A., Tilton, R.D., Sholl, D.S., Lowry, G.V., 2005b. TCE Dechlorination Rates, Pathways, and Efficiency of Nanoscale Iron Particles with Different Properties. *Environ. Sci. Technol.* **39**, 1338-1345.
- Luepin, O.X., Hug, S.J., Badruzzaman, A.B.M., 2005. Arsenic Removal from Bangladesh Tube Well Water with Filter Columns Containing Zerovalent Iron Filings and Sand. *Environ. Sci. Technol.* **39**, 8032-8037.
- Matheson, L., Tratnyek, P., 1994. Reductive Dehalogenation of Chlorinated Methanes by Iron Metal. *Environ. Sci. Technol.* **28**, 2045-2053.
- Milazzo, G., Caroli, S., Sharma, V.K., 1978. *Tables of Standard Electrode Potentials*. London, England: Wiley.
- Morrison, S.J., Metzler, D.R., Carpenter, C.E., 2001. Uranium Precipitation in a Permeable Reactive Barrier by Progressive Irreversible Dissolution of Zerovalent Iron. *Environ. Sci. Technol.* **35**, 385-390.
- Nurmi, J.T., Tratnyek, P.G., Sarathy, V., Baer, D.R., Amonette, J.E., Pecher, K., Wang, C., Linehan, J.C., Matson, D.W., Penn, R.L., Driessen, M.D., 2005. Characterization and Properties of Metallic Iron Nanoparticles: Spectroscopy, Electrochemistry, and Kinetics. *Environ. Sci. Technol.*, **39**, 1221 – 1230.
- Orth, W.S., Gillham, R.W., 1996. Dechlorination of Trichloroethene in Aqueous Solution Using Fe<sup>0</sup>. *Environ. Sci. Technol.* **30**, 66-71.

- Phillips, D.H., Gu, B., Watson, D.B., Roh, Y., Liang, L., Lee, S.Y., 2000. Performance Evaluation of a Zerovalent Iron Reactive Barrier: Mineralogical Characteristics. *Environ. Sci. Technol.* **34**, 4169-4176.
- Ponder, S.M., Darab, J.G., Mallouk, T.E., 2000. Remediation of Cr(VI) and Pb(II) Aqueous Solutions Using Supported, Nanoscale Zero-valent Iron. *Environ. Sci. Technol.* **34**, 2564-2569.
- Potter, T.L., Carpenter, T.L., 1995. Occurrence of Alachlor Environmental Degradation Products in Groundwater. *Environ. Sci. Technol.* **29**, 1557-1563.
- Quinn J., Geiger C., Clausen C., Brooks K., Coon C., O'Hara S., Krug T., Major D., Yoon W.S., Gavaskar A., Holdsworth T., 2005. Field demonstration of DNAPL dehalogenation using emulsified zero-valent iron. *Environ Sci Technol.* **39**, 1309–1318.
- Radig, S., 1997, Updated 2006. North Dakota Geographic Targeting System for Groundwater Monitoring. North Dakota. Department of Health, Division. of Water Quality. Retrieved November 16, 2006 from <http://www.health.state.nd.us/WQ/GW/pubs/GWT.HTM>.
- Rock, M.L., Kearney, P.C., Helz, G.R., 1998. Innovative Remediation Technology. In P.C. Kearney., T. Roberts (Eds.) *Pesticide Remediation in Soils and Water* (pp. 1-19) West Sussex, England: Wiley.
- Saleh, N, Kim H.J., Matyjaszewski, K., Tilton, R.D., and Lowry, G.V., 2008. Ionic Strength and Composition affect the mobility of surface-modified NZVI in water-saturated sand columns. *Environ. Sci. Technol.* **42**, 3349-3355.
- Saleh, N., Sirk, K., Liu, Y., Phenrat, T., Dufour, B., Matyjaszewski, K., Tilton, R., Lowry, G. V., 2007 Surface Modifications Enhance Nanoiron Transport and DNAPL Targeting in Saturated Porous Media. *Environ. Eng. Sci.* **24**, 45-57.
- Saleh, N., Phenrat, T., Sirk, K., Dufour, B., Ok, J., Sarbu, T., Matyjaszewski, K., Tilton, R., Lowry, G. V., 2005. Adsorbed Triblock Copolymers Deliver Reactive Iron Nanoparticles to the Oil/Water Interface. *Nano Lett.* **5**, 2489-2494.
- Sigma-Aldrich, Inc., 2007. Specification Sheet #267953 and Personal Communication
- USDA (United States Department of Agriculture), 2007. *The ARS Pesticide Properties Database*. US Department of Agriculture, Agricultural Research Service. Retrieved 11/01/2007 from <http://www.ars.usda.gov/Services/docs.htm?docid=14199>
- Villas-Horns, C., Minnesota Department of Agriculture, Pesticide and Fertilizer Management Division, (Personal Communication). 2006.

- Weber, E., 1996. Iron-Mediated Reductive Transformations: Investigation of Reaction Mechanism. *Environ. Sci. Technol.* **30**, 716-719.
- Wilkin, R.T., Su, C., Ford, R.G., Paul, C.J., 2005. Chromium Removal Process during Groundwater Remediation by Zerovalent Iron Permeable Reactive Barrier. *Environ. Sci. Technol.* **39**, 4599-4605.
- Zhang, W., 2003. Nanoscale Iron Particles for Environmental Remediation: An Overview. *J. Nanopart. Res.* **5**, 323-332.